Flight Effects on Turbofan Fan Tones

Eric Nesbitt[1], Ian A. Clark[2], Yueping Guo[3] and Russell H. Thomas[4]
NASA Langley Research Center, Hampton, VA 23681, USA

This paper presents a summary and status of the ongoing development of an all-new fan tone noise prediction process. This process is being developed based on data from both the Quiet Technology Demonstrator 2 (QTD2) and the NASA/Boeing Propulsion Airframe Aeroacoustics & Aircraft System Noise (PAA/ASN) tests. The fan tone prediction model development steps are outlined, and rationale for a framework is provided. The two most significant findings of this work are how the fan tone noise correlates best with relative tip Mach number and the change in the directivity of the inlet tone noise relative to the aft. Using the framework, an initial proposed model has been developed which reduces the overall fan tone noise prediction miss on a power-level basis from +/- ~25dB to +/- ~5dB. This is expected to greatly improve the ability to predict both current and future aircraft concepts.

I. Nomenclature

θ	=	Emission Angle – Relative to the inlet axis
SPL	=	Sound Pressure Level dB – Relative to p_0
bbspl	=	Broadband SPL
nbspl	=	Narrowband SPL
tnspl	=	Tone SPL
BPF	=	Blade Passage Frequency
p_0	=	$2\text{x}10^{-5}$ Pascals
W_0	=	$1\text{x}10^{-12}$ Watts
ρ_0	=	0.00129 g/cm^3
c_0	=	33100 cm/s
r	=	1 ft (30.48 cm)
n	=	n^{th} fan harmonic tone
tnSPLn	=	Tone SPL for the n^{th} harmonic fan tone
PAAcor	=	Propulsion Airframe Aeroacoustic correction
tnPWRn	=	Tone Power Level over a defined arc ($\theta_2 - \theta_1$) for the n^{th} fan harmonic
iso	=	Corrected to an isolated engine state
F3(θ)	=	Normalized directivity as a function of θ
$F_4(n)$	=	Function for higher harmonics
m	=	Mass flow rate lb/sec (kg/sec)
m_o	=	Reference flow rate. 1 lb/sec (.453 kg/sec)
M	=	Airplane Mach number
Mrel	=	Fan tip relative Mach number
MrelADP	=	Fan tip relative Mach number at the Aero Design Point
RSS	=	Rotor stator spacing divided by fan blade chord, %
θ_{ref}	=	Reference inlet and aft arc angle for use in convective ampification term

[1] Senior Research Engineer, Aeroacoustics Branch, AIAA Senior Member, Eric.H.Nesbitt@nasa.gov
[2] Research Aerospace Engineer, Aeroacoustics Branch, AIAA Senior Member, Ian.A.Clark@nasa.gov
[3] Senior Research Engineer, Aeroacoustics Branch, AIAA Associate Fellow, Yueping.Guo@nasa.gov
[4] Senior Research Engineer, Aeroacoustics Branch, AIAA Associate Fellow, Russell.H.Thomas@nasa.gov

ΔT = Total temperature rise across the fan, $^{\circ}R$, K
ΔT_o = Reference fan total temperature rise, 1 $^{\circ}R$ (.555 K)
AE = Effective area of the fan nozzle (ft^2)
AE_o = Reference effective area of fan nozzle (1 ft^2)

II. Introduction

In the ever-evolving landscape of aviation, the demand for quieter and more efficient aircraft has become paramount. High bypass ratio turbofans have emerged as the dominant propulsion system, exhibiting significant fuel efficiency, and reduced environmental impact. As these engines have become increasingly prevalent, understanding and mitigating the noise generated by their operation is an ongoing challenge.

Among the various aspects of fan tonal noise, the detailed understanding of flight effects is an important factor in the design of these types of aircraft. In this context, the flight effects refer to the dependence of the acoustic radiation on all aspects of how the fan tone noise propagates in a full-scale flight environment. These characteristics are particularly relevant in understanding the noise impact experienced by communities surrounding airports and in the development of effective noise reduction strategies.

The fan, as a primary noise source in high bypass ratio turbofans, is subjected to complex aerodynamic and acoustic interactions that are (at least) a function of fan design, flow conditions and operating parameters. Airspeed is a critical aircraft operating variable, and understanding if and how fan noise characteristics are affected by it is important for predicting and controlling fan noise. The installation aspects are important as well, and an understanding of the source in addition to Propulsion Airframe Aeroacoustic (PAA) effects will also be explored in detail in this paper.

This paper will present turbofan noise data from full-scale flight testing of high bypass ratio turbofans relative to a newly developed proposed prediction and compare that to the current state-of-the-art predictions. The paper will present predictions relative to data from both the Propulsion Airframe Aeroacoustics and Aircraft System Noise flight research (PAA/ASN) test completed in 2020 [1]-[2] and from the Quiet Technology Demonstrator 2 (QTD2) test completed in 2005 [3]. It is important to note that in the PAA/ASN test the airplane was powered by a GEnx-1B production engine. In the QTD2 test, the airplane was powered by a GE90-115B engine, and the configuration being used in this analysis is the non-production Acoustically Smooth Inlet (ASI) with a hardwalled lip. Since there is a significant amount of proprietary data being used as part of this study and current agreements restrict its release, there will be illustrative cartoons used extensively in place of actual data plots. However, the paper will delve into the methodology employed, present the results relative to current predictions, discuss the status of the investigation, and finally discuss implications for both the research community and industry.

III. Prediction Framework

As the title of the paper suggests, when this work was initially conceived the plan was to show how the data sets compared to the current NASA fan tone noise prediction [4] and discuss the differences likely created by affects associated with the full-scale flight testing. As the work progressed however, it became clear that a completely different process was needed. Although the reasoning and the supporting data will be shown later, this section will present the overall framework. Previous fan tone noise methods [4]-[8] have typically used the peak level in the correlation for the tones. However, when dealing with fan tonal noise from full-scale flight testing this is practically impossible due to the highly lobular nature of the fan tonal noise. The highly lobular nature means that picking the "peak" radiation angle would be significantly variable and would likely create much more scatter in the analysis than is truly supported by the data. For this reason the data are normalized to a 1ft polar arc lossless basis and a power level calculated over a defined arc. Thus the framework is simular to the process as used by Nesbitt, et al. [9] and is shown in Fig. 1.

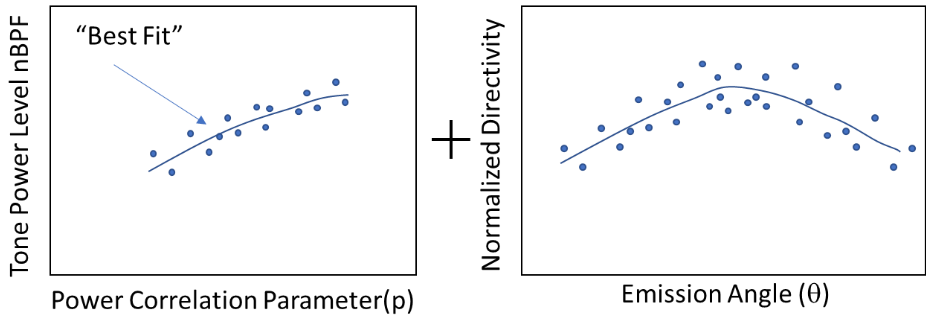

Fig. 1 Prediction Framework for fan tone noise from full-scale flight testing.

Where:

$$tnSPLn(p,\theta)_{iso} = tnPWRn(p)_{iso} + [tnspl(\theta)_{iso} - tnPWRn(p)_{iso}] \tag{1}$$

and:

$$tnspl(\theta)_{iso} = tnSPLn(\theta)_{flyover\ array} - PAAcor \tag{2}$$

$$tnPWRn(p)_{iso} = 10log\left\{\frac{2\pi\frac{r^2p_0^2}{\rho_0c_0}\sum_{i=\theta1}^{\theta2}[10^{tnSPLni_{iso}/10}]\,sin\theta_i\,\Delta\theta}{W_0}\right\} \tag{3}$$

and:

$$[tnSPL(\theta)_{iso} - tnPWRn(p)_{iso}] = F3(\theta) \tag{4}$$

The research presented here is the first time full-scale acoustically treated flight test data have been used in the development of a fan noise prediction process for eventual inclusion in the NASA ANOPP prediction process. This is expected to greatly improve the accuracy of the prediction for two primary reasons. First, it removes the uncertainties associated with using either model-scale data and/or static test stand data (which has been used to date) and these uncertainties are always largest on the fan tones. Second, it reduces the uncertainty of predicting the absolute value of the tone attenuation, which is very difficult without detailed source information [10]. Detailed fan source information is almost never available and not even possible to get with an early airplane development-type prediction. Instead, the prediction process will predict the level of a treated baseline where the baseline is a defined type and amount of treatment. All that remains then for any prediction of any given geometry is to predict the delta attenuation. This will always be a smaller number and therefore result a lower level of uncertainty.   The use of treated full-scale data also means there is no significant contribution of Multiple Pure Tone (MPT - or "Buzzsaw") noise in the data at supersonic tip speeds. This was noted as an issue in the development of the current model [4]. This also means there will be no attempt to predict the MPT noise as it is not a significant contributor in the modern turbofans being used for this study. Further details of the data analysis shown will be discussed in detail in the next section.

IV.   Data Analysis Procedure

The data used as input to this process are in the form of ensemble-averaged narrowband data from ground plane microphone arrays arranged as shown in Fig. 2. These data (processed and normalized by Boeing per the method described in [11]) are used by NASA to perform further analysis and will be discussed below.

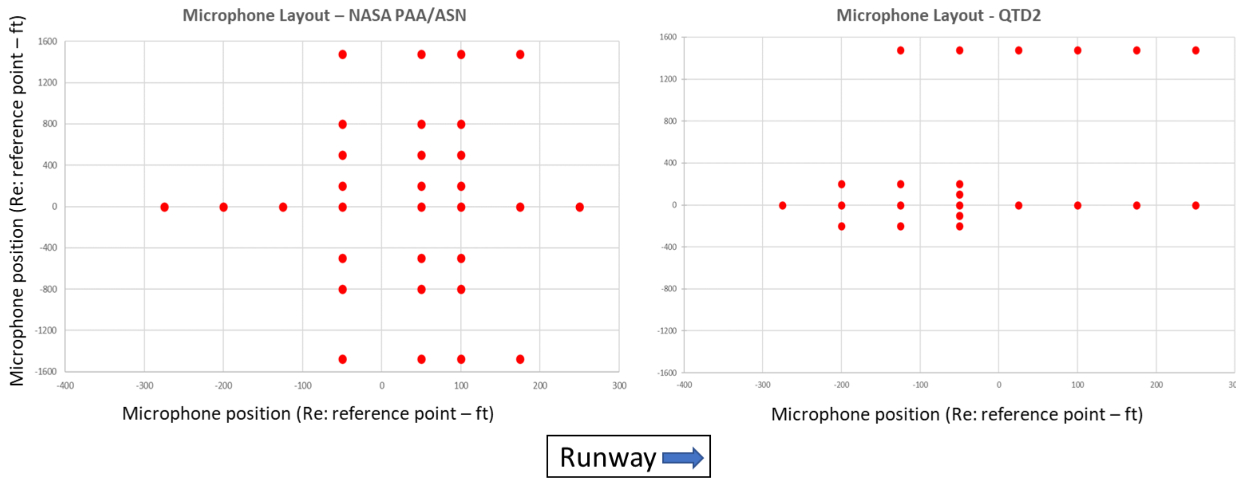

Fig. 2 Farfield microphone layouts from the flight tests.

The first important step to identify and extract the fan tones from the total noise is to remove the Doppler frequency shift from the data. The Doppler frequency is calculated using the original flight Mach number for each condition and the emission angle relative to the engine centerline as provided by Boeing. The data are then interpolated to a zero-Mach number frequency. The engine centerline angle is used, since it is held constant in the data normalization process Boeing employs. The emission angle relative to the flight path (which would be the more correct angle) has an unknown relationship to the original flight path, because the data are all normalized to a common flight path. This issue causes some small uncertainty in the analysis and can result in tone levels being a bit smeared in frequency over the flyover.

Once the data have been deDopplerized and the tones are nominally at the same frequency for the flyover, the tones and broadband must be separated. To do this first, a good estimate of the broadband is needed. Initially a simple median filter [12] was used as shown in Fig. 3a. As the figure shows the "broadband" noise still contains many "haystacks" in the narrowband data. Although the fan tone levels are being extracted close to the correct value, the many "haystacks" when summed into 1/3 octave bands results in spectra that appear to have tones in them. Even though the fan tone levels are approximately correct, there is a desire to also extract the fan broadband noise for use in the broadband prediction development described in the companion paper [13]. To do this the median filter output is put through the "minimum broadband" algorithm as described by Nesbitt, et al. [9]. This algorithm traces the lower bounds of the input spectra. By doing this with the output of the median filter, the "haystacks" are effectively removed from the spectra and a more true broadband results. This is the first time (as far as the authors are aware) these two algorithms for broadband identification have been used in tandum for a good median estimate of the broadband noise without including the "haystacks."

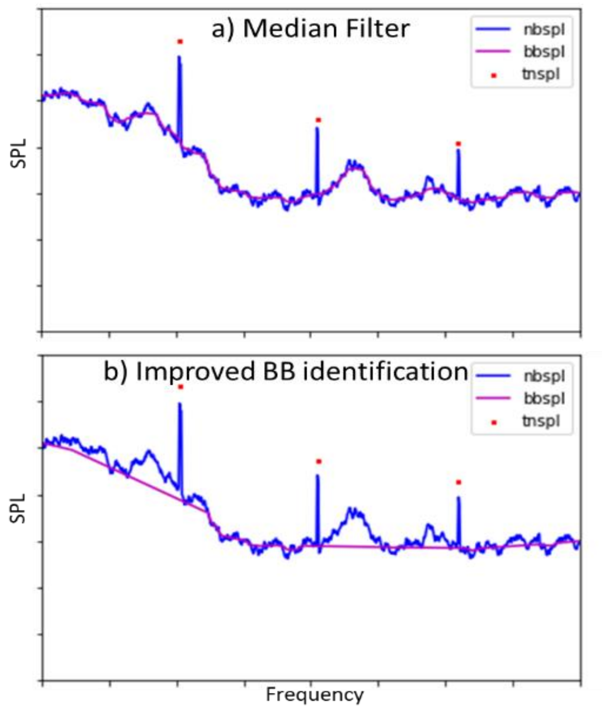

Fig. 3 Sample of tone extraction from broadband using randomly generated narrowband spectra.

After the broadband noise is identified, the tones are extracted. This involves summing the fan tone energy over a defined tone stencil with a defined tone emergence and subtracting the summed broadband noise over the same stencil. This method is further illustrated in Fig. 4.

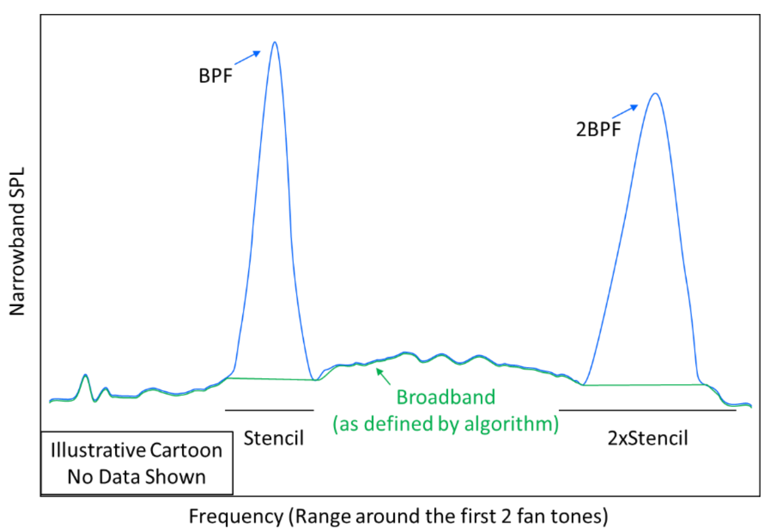

Fig. 4 Tone separation process illustration.

The tone stencil center frequency is predicted from the fan RPM (provided by Boeing with the data) and the known blade count. The width of the stencil is input into the process based on how smeared in frequency the tones appear. The tone stencil method is used due to the uncertainties in the deDopplerization as described above and is needed to capture total tone energy even if the tone is somewhat "smeared" in frequency. Figure 3b shows a sample of the tone extraction method using a random-number-generated (but representative) spectrum. As the figure shows, the method successfully extracts and accounts for the fan broadband and tonal noise.

Once the tone levels as a function of emission angle are obtained, the data need to be corrected to an “isolated” state (i.e., corrected for PAA effects). The data from the flyover microphones are used in this study (microphones on the zero y-axis from Fig. 2) because the objective is to keep the PAA effects at a minimum. Even though the PAA effects are expected to be relatively small for the flyover plane, they do need to be backed out of the data. To do this, a data-driven method is used. Ultimately the plan is to use the method by Guo [14] to correct for PAA effects, but for now the method uses experimental results from the Boeing Low Speed Aeroacoustic Facility [15]. The output of this process results in as close to isolated fan tone noise as can be resonably obtained from the full-scale flight test data.

At this point, full-scale “isolated” fan tonal data from two different engine types have been obtained. However, the data are not separated into forward and aft radiated and the two sets of data include acoustic treatment of differing amounts. The first step to address these issues is to separate the data into forward and aft arcs using the hardwall and treated fan duct data from the PAA/ASN flight test. The inlet arc angular range is chosen such that when summed into a power level over the arc there is no discernible difference between the hardwall and treated fan duct configurations. The aft arc angular range is then chosen based on engineering judgement by looking at where the attenuation is not yet dropping significantly. This indicates the levels are likely to be completely dominated by the aft-radiated fan noise. The angular ranges chosen for this study and an illustration of how the tone levels vary in flight are shown in Fig. 5.

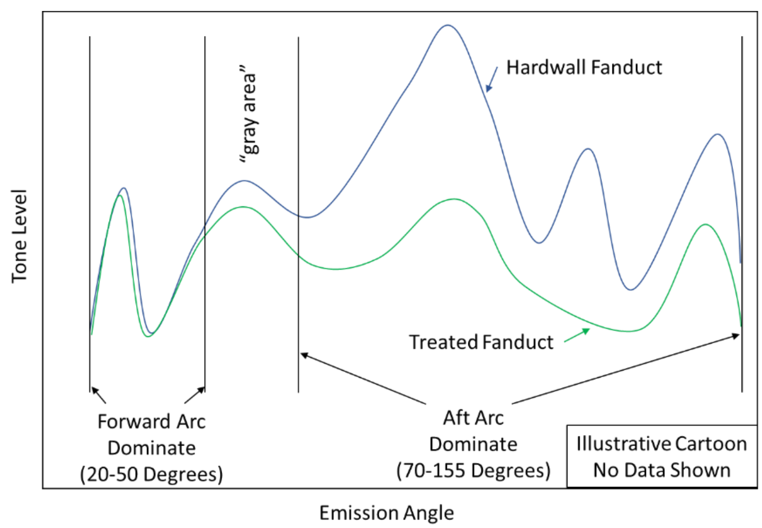

Fig. 5 Illustration of forward and aft-radiated fan tonal noise.

As the illustration in Fig. 5 depicts, fan tonal noise is generally very lobular in nature (particularly in flyover testing) and using just the shape of the directivity to separate the inlet and aft-radiated noise (as is sometimes used for broadband noise [9]) is practically impossible. The cartoon also shows a “gray area” where both the inlet and aft arc contibute to the total fan noise level. For the purposes of the power-level analysis this area is excluded and the sound energy in it will be accounted for later in the development of the directivity functions.

Once the forward and aft-arc power levels are defined, the data still needs to have lining corrections applied. The method used for predicting acoustic attenuation for this was the General Electric (GE) method developed by Kontos et al. [16]. As discussed by Clark et al. [17], liner technology has developed significantly since the model development 25 years ago. That said, the method is assumed to work well for predicting the effects of the amount of lining when the liner technology is relatively the same as in this case. Figure 6 shows the predicted attenuation for the forward and aft-arc peak angles for both cases. As previously stated, it is the difference between the lines in Fig. 6 that is applied to the data and at the respective tone frequencies to result in data sets with nominally the same amount of treatment of a similar design.

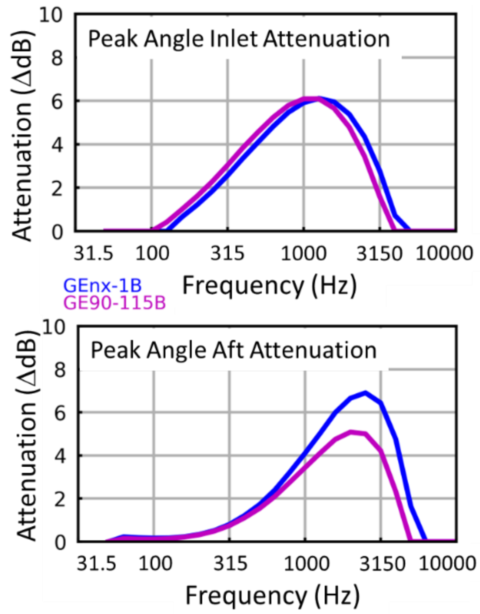

Fig. 6 Predicted attenuation at the peak Inlet and Aft angles.

The data are now corrected to the same amount of lining and power levels as calculated per Eq. (3). There is still the desire however to compare to the hardwall predictions of Krejsa [4]. In order to do this, total tonal attenuation is needed. As previously stated, the calculation of total tonal attenuation (in particular) is very inaccurate and could lead to conclusions that would relate to the lining prediction as opposed to the basic correlation being explored here. In order to address this, a data-driven approach is used.

For the aft arc and for the GEnx-1B engine hardwall fan noise was measured in the PAA/ASN test and therefore is not an issue. For the aft arc and for the GE90-115B engine measured in QTD2, the measured attenuations from the PAA/ASN test were correlated to relative tip mach number, corrected for the amount of lining difference (using the GE method [16]), and applied to the aft tone data to give a best estimate of the hardwalled aft-arc fan tone noise.

There were no measurements in either test of a hardwalled inlet. However, there are tone attenuation measurements from the QTD3 test [18], which NASA has access to. In order to correct the inlet data a similar process was used, where the measured QTD3 tone attenuations were correlated to relative tip mach number, corrected for the amount of lining difference (again using the GE method [16]), and applied to the inlet tone data to give a best estimate of a hardwalled inlet.

It should be emphasized that the lining attenuations being used are only to compare to the existing predictions in a consistant manner without adding the uncertainty of a tone attenuation prediction.

V. Fan Tone Power-Level Prediction Development

As previously discussed, as the work progressed it became clear that a completely different fan tone noise process was needed. The reason for this is illustrated in Fig. 7.

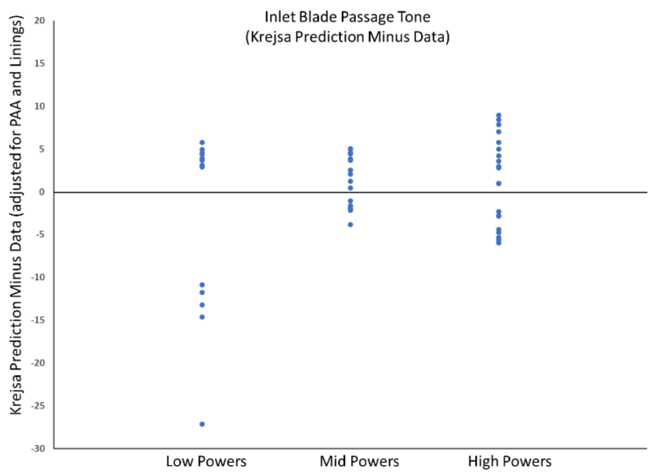

Fig. 7 Difference (Krejsa prediction minus data) Inlet BPF tone.

As Fig. 7 shows, there is approximately a plus 10 dB minus 30 dB over and underprediction of the inlet BPF tone, and the differences seem to be a strong function of power setting. Although presented in a different form, this is consistent with the results shown by Clark, et al. [17]. This suggests that there is likely more going on than the PAA effects and other effects associated with full-scale flight testing. Instead there is likely an issue with the basic correlation. The correlation used in the inlet-radiated tone prediction of Krejsa[4] (shown here for completeness) is:

$$SPL(f,\theta)_{@1Meter} = 10\ log_{10}(m/m_o) + 40\ log_{10}(\Delta T/\Delta T_o) + 42 - 20M_{rel} - 10log_{10}(RSS/300) + F_3(\theta) + F_4(n) \quad (5)$$

and for the aft-radiated tone prediction:

$$SPL(f,\theta)_{@1Meter} = 10\ log_{10}(m/m_o) + 40\ log_{10}(\Delta T/\Delta T_o) + 34 - 17(M_{rel} - .65) - 10log_{10}(RSS/300) + F_3(\theta) + F_4(n) \quad (6)$$

Looking closely at Eqs. (5) and (6) there are two significant issues that may be contributing to the poor prediction. First, there are really two different parameters that are a function of engine power and they appear to "fight" each other (i.e., have opposite signs). These are the total temperature rise across the fan and the fan tip relative Mach number. Secondly, it should be noted that the the relative tip Mach number is used directly without a $\log_{10}$ function. This is puzzling and there is no explanation as to the reasoning put forth in the reference material [4] and it is different than what was used in the Heidmann prediction [5], which was the main starting point for Krejsa [4]. To address these issues with the engine power correlation, a somewhat different form of the correlation is proposed:

$$tnPWRn_{@1ft} = 10\ log_{10}(AE/AE_o) + A\ log_{10}(M_{rel}) + B\ log_{10}(M_{rel}ADP) + C\ log_{10}(1-Mcos(\theta_{ref})) + D\ log_{10}(RSS/300) + E + F_4(n) \quad (7)$$

The tone power level is then predicted with Eq. (7) and used in Eq. (1) and the tone level at any angle (θ) can be predicted. The exponents (constants) in Eq. (7) (A, B, C, D and E) are then derived using a multiple linear regression where the objective function is set to make the R-squared be a value of 1. This is done using the evolution optimization function within SciPy [19] with limits set to keep the values of the exponents reasonable. This is then done separately for both the inlet and aft-radiated noise. It should be noted in Eq. (7) there is only the fan relative tip Mach number and an addition of a design fan relative tip Mach number, which is a constant for a given fan design, meaning there now is just one term to account for the effect of engine power. When looking at the normalized data from the two tests included in this study it became very apparent that the relative tip Mach number was a significantly better parameter than the total temperature rise across the fan to account for the effect of engine power. Finally Eq. (7) is defined separately for both the BPF and 2BPF and then the F4(n) function is used to account for higher harmonics. The reason for this is that getting an accurate level of the higher harmonics from the treated flight test data was practically impossible due to signal-to-noise issues and the tones dropping into the surrounding broadband.

In addition, since the flight test data used in this study contain conditions of differing aircraft speeds, the convective amplification term is included in the optimization. Also, since the optimization was done on a power-level basis, a reference angle (i.e., the mid-point of the integration) was used. The inclusion of the convective amplification term significantly improved the correlation especially for the inlet-radiated noise.

Finally to correct for the overall size of the fan, the effective area of the fan nozzle is being used instead of the mass flow. Although for a given engine the effective area and mass flow have an almost linear relationship, the effective area appeared to work somewhat better and was a more intuitive parameter and therefore has been chosen in this case.

VI. Fan Tone Directivity Development

The directivity function is the next thing to consider. The tone deltas as defined in Eq. (4) are calculated and plotted as a function of emission angle (θ). Due to the previously discussed lobular nature of the tonal noise there is significant data scatter. For a low-order prediction as is being developed here there is no chance the lobes can be effectively predicted. The first issue becomes how to define a directivity function that, on an average basis, gets the overall trend of the data. The second issue is how to deal with the "gray area" defined in Section IV as the angular range where both the inlet and aft-radiated fan tone noise are contributing significantly. How these issues are accounted for will now be described in detail.

First the data are broken into sub- and supersonic groupings. This comes from examining the data and determining where the directivity shapes are significantly different for these different fan speed regimes. This is expected, as the source of the fan tone noise changes when the rotor-locked field cuts on at supersonic speeds.

Secondly a third-order least square curve fit was put through the data over the defined arc. This then allowed for a prediction interval to be calculated and the data scatter quantified. For the data used in this study the 80% prediction interval was typically +/- ~5 dB. This means there is an 80% chance a future measurement would be within this range.

Finally, the "gray area" needs to be defined such that when the forward and aft arcs are summed there is neither undue sound energy gained or lost. This is an area where this development is not currently finished in that there have been slopes defined for the forward and aft arcs outside of the defined curve fit windows and spot checks have been done for the BPF only, but a comprehensive study of this will need to be done and the slopes adjusted before the prediction process could be considered ready to use. Figure 8 shows an illustration of the process used to define the directivity functions for the inlet arc.

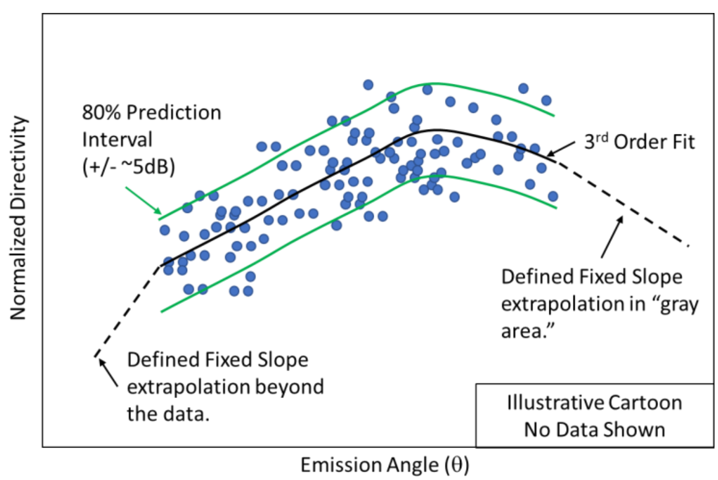

Fig. 8 Illustration of the process used to define the inlet directivity functions.

The directivity development process has now produced a total of eight different directivity functions. For both the BPF and 2BPF there are forward and aft-arc functions for both subsonic and supersonic conditions. A set of comparisons of these directivity functions to the current model will be shown in the next section.

VII. Summary of Results

This section outlines results analyzed and includes effects on the BPF and 2BPF tones and will present how the fan tone power levels and directivities compare to the current process and to the proposed process. Figure 9 shows the results of the analysis for the inlet arc BPF. Note that Fig. 9a is the same as Fig. 7 and is shown here again for a side-by-side comparison. As shown, the proposed prediction relative to the data reduces the overall prediction miss to within +/- ~5 dB. This is a significantly large improvement over the current process!

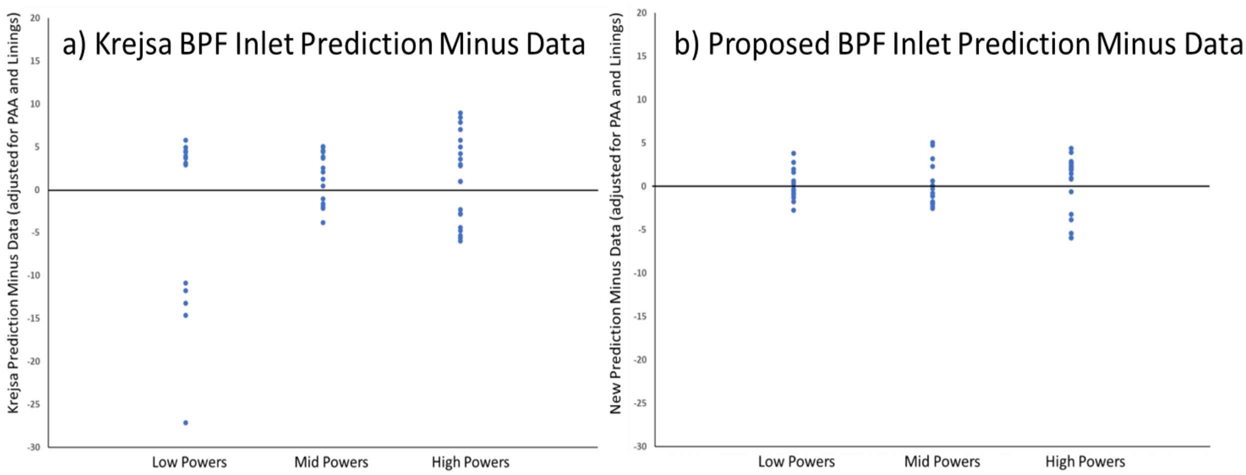

Fig. 9 Inlet arc BPF power-level prediction comparisons to data.

Figures 10-12 show the same type of comparisons for the aft arc BPF, inlet 2BPF and aft 2BPF. As the figures show there is again a dramatic improvement, with the predictions going from approximately +/- 20+ dB under and overprediction to approximately +/- 5 dB.

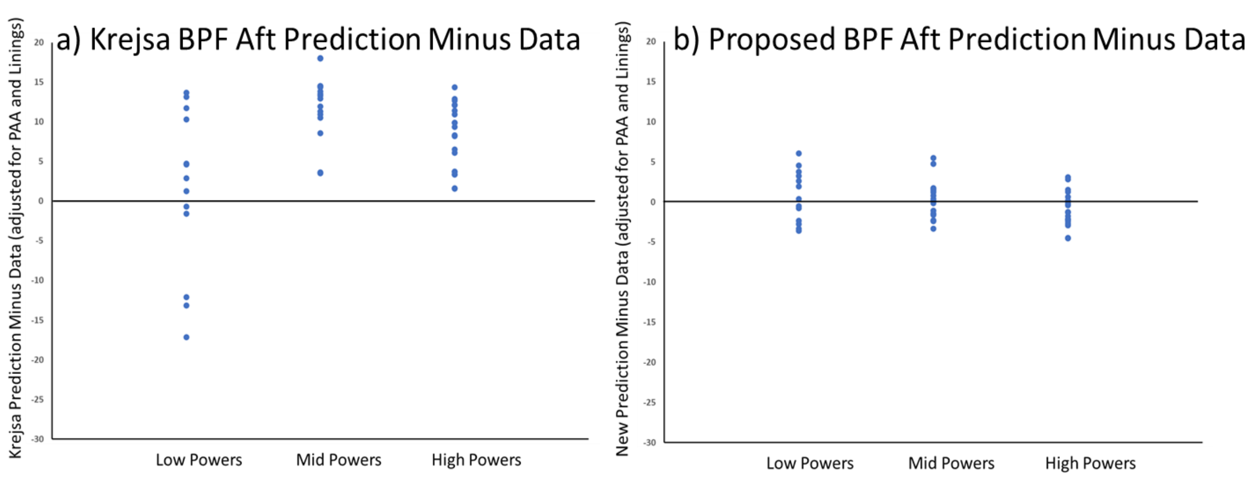

Fig. 10 Aft arc BPF power-level prediction comparisons to data.

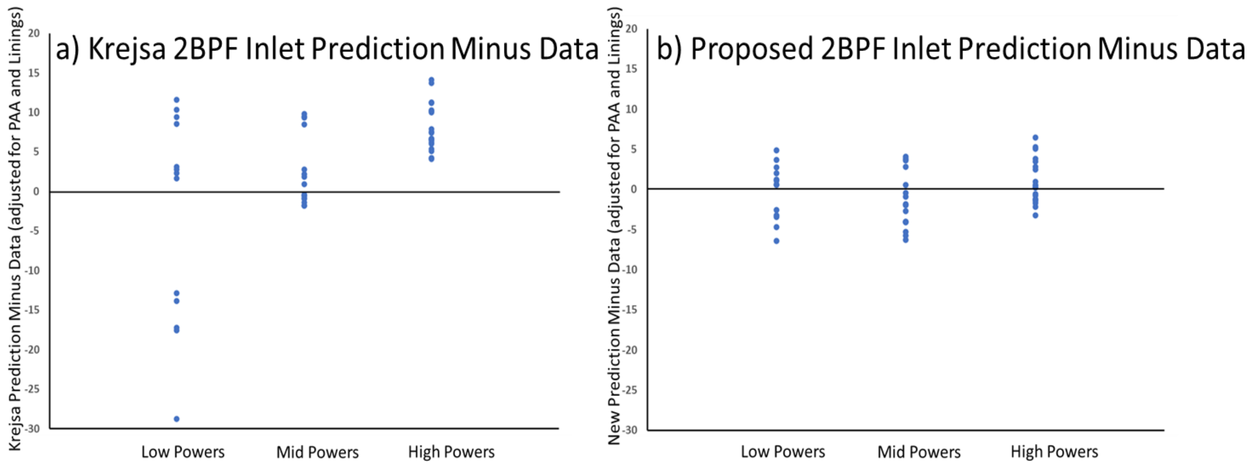

Fig. 11 Inlet arc 2BPF power-level prediction comparisons to data.

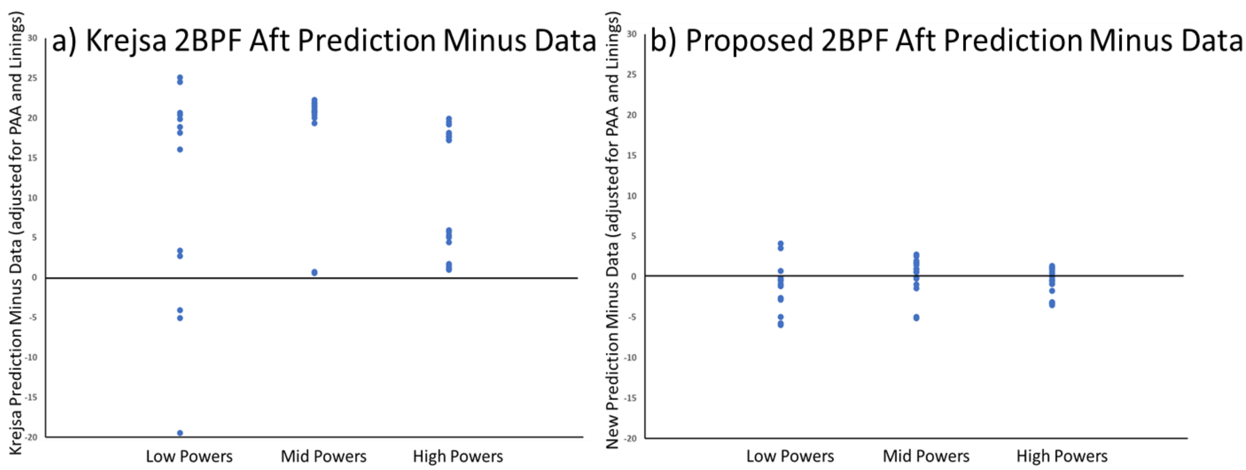

Fig. 12 Aft arc 2BPF power-level prediction comparisons to data.

The directivity functions developed using the process described in the last section will now be presented relative to the directivity functions of Krejsa [4]. Figure 13 shows these comparisons for BPF, where the peaks of the directivity functions have been normalized to zero for both to better show how the shapes compare. As noted earlier, particularly in the "gray area," the curves presented should be considered preliminary and will be revised once the total energy issue is resolved.

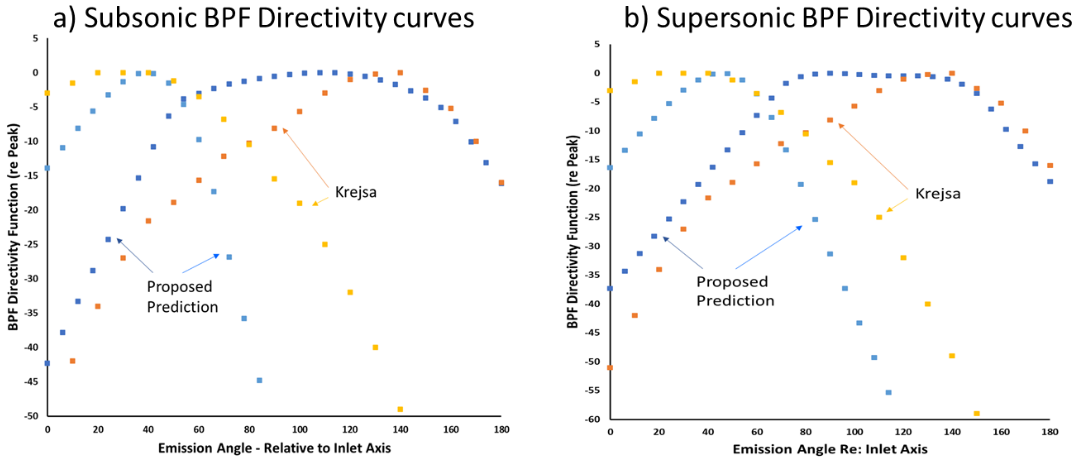

Fig. 13 BPF directivity functions compared to those of Krejsa

That said, looking closely at Fig. 13 there are a couple things of note. First, the most notable issue is the aft arc noise is more dominant significantly further forward than in the current prediction. The main reason for this is likely due to the current predictions [4] being made using hardwall model-scale data. The presence of the acoustically smooth inlet likely reduces the relative importance of inlet tone noise particularly in the mid angles. This will mean inlet tone noise will be of less total importance in the proposed predictions and the aft arc tone noise will control more of the total fan noise.

Secondly, it is clear the shapes of the directivity functions are different for the cases shown – even though in the current predictions there are no differences. (i.e., the Krejsa curves in the plots are the same). This was noted by Krejsa as an issue [4], but at the time it was felt the trends were not clear enough to justify different curves. This is another area where the use of full-scale treated flight test data makes this possible due to the absence of any significant MPT noise.

VIII. Conclusions and Future Work

This is the first time full-scale acoustically treated turbofan flight test data have been used in the development of a fan noise prediction process for eventual inclusion in the NASA ANOPP prediction process. The process for analyzing and predicting fan tonal noise from flight test results has been defined and used to compare to current predictions. The prediction miss on a power-level basis has been reduced from +/- ~25 dB to +/- ~5 dB. This is a very large improvement. Even considering the additional +/- ~5 dB of uncertainty on the directivity functions, the overall prediction uncertainty is expected to be ~+/-7 dB. This is within the typical data scatter seen in the tone data from full-scale flight testing. That said, it is important to understand that there is much to be done before this prediction process can be released.

The first issue to be worked is to finish the directivities. This will clarify and correct for any issue that is apparent with either losing or gaining acoustic energy in the "gray area" of the directivity where both the inlet and aft-radiated noise contribute significantly to the total. To do this, the inlet and aft arc will separately be predicted, added, and compared to the total measured directivity and power level. If there is an issue, then the results from phased array measurements (which were taken in both tests used as part of this study) will be used to improve and help develop final directivity functions. Secondly, there would be added value to extend the validation of this prediction with an independent data set that was not used in its development. Recognizing there are significant challenges, options for a path forward are being considered.

The implications of this work are significant. It is emphasized that the proposed model formulations have been created using research-quality data from a highly relevant full-scale flight test on a state-of-the-art aircraft with modern engines and have been shown to exhibit strongly improved characteristics relative to prior system-level fan noise prediction methods. It is expected that the models presented in this work represent a significant improvement in the ability of NASA to predict fan tone noise for both current in-service aircraft and future aircraft concepts.

This work, along with the companion paper on broadband, has the potential to improve both the prediction accuracy and fidelity. The accuracy improvement is obvious from the data presented, but the fidelity (i.e., the ability of the prediction to correctly predict the effects of changes to designs) is also improved due to the improvement in the engine power correlation. Although for a given fan design it is true that the rise in temperature across the fan and the fan relative tip Mach number have a linear relationship, this is not true if the design of the fan is changed. This proposed process will now more correctly predict changes of this nature, which is significant in the product development of an airplane.

Acknowledgments

Funding for this research by the NASA Advanced Air Transport Technology Project is gratefully acknowledged. The exceptional efforts of The Boeing Company and the Boeing ecoDemonstrator Program are gratefully acknowledged in the execution of the tests and the delivery of the data used in this study.

References

[1] Thomas, R. H., Guo, Y., Clark, I., and June, J., "Propulsion Airframe Aeroacoustics and Aircraft System Noise Flight Research Test: NASA Overview," AIAA Paper 2022-2993, 28th AIAA/CEAS Aeroacoustics Conference, Southampton, UK, June 14-17, 2022. doi: 10.2514/6.2022-2993.

[2] Czech, M., Thomas, R. H., Guo, Y., June, J., Clark, I., and Shoemaker, C., "Propulsion Airframe Aeroacoustics and Aircraft System Noise Flight Test on the Boeing 2020 ecoDemonstrator program," AIAA Paper 2022-2994, 28th AIAA/CEAS Aeroacoustics Conference, Southampton, UK, June 14-17, 2022. doi:10.2514/6.2022-2994.

[3] Herkes, W. H., Olsen, R. F., and Uellenberg, S., "The Quiet Technology Demonstrator Program: Flight Validation of Airplane Noise-Reduction Concepts," AIAA Paper 2006-2720, 12th AIAA/CEAS Aeroacoustics Conference, Cambridge, Massachusetts, May 8-10, 2006. doi: 10.2514/6.2006-2720.

[4] Krejsa, E. A. and Stone, J. R., "Enhanced Fan Noise Modeling for Turbofan Engines," NASA CR-2014-218421, 2014. URL https://ntrs.nasa.gov/citations/20150000884.

[5] Heidmann, M. F., "Interim Prediction Method for Fan and Compressor Source Noise," NASA TM X-71763, 1979. URL https://ntrs.nasa.gov/citations/19750017876

[6] Kontos, K. B., Janardan B. A., and Gliebe, P. R., "Improved NASA-ANOPP Noise Prediction Computer Code for Advanced Subsonic Propulsion Systems, Vol. 1: ANOPP Evaluation and Fan Noise Model Improvement," NASA CR 195480, August 1996. URL https://ntrs.nasa.gov/citations/19960048499

[7] Hough, J. W. and Weir D. S., "Aircraft Noise Prediction Program (ANOPP) Fan Noise Prediction for Small Engines," NASA CR 198300, April 1996. URL https://ntrs.nasa.gov/citations/19960042711

[8] Herkes, W., "Modular Engine Noise Component Prediction System (MCP) Technical Description and Assessment Document," The Boeing Company, NASA Contract NAS1-97040, August 2001.

[9] Nesbitt, E. H., Ganz, U. W., Diamond, J. A., and Kosanchick, M. III, "An Empirical Prediction of Inlet Radiated Broadband Noise from Full Scale Engines," AIAA Paper 1998-0470, 36th AIAA Aerospace Sciences Meeting and Exhibit, Reno, Nevada, January 12-15, 1998. doi: 10.2514/6.1998-470.

[10] Zlavog, G., and Eversman,W., "Source effects on attenuation in lined ducts. Part I: A statistically based computational approach," Journal of Sound and Vibration, Vol. 307, No. 1, 2007, pp. 113–138. doi:10.1016/j.jsv.2007.06.031.

[11] Czech, M. J., Uellenberg, S., Nesbitt, E., and Abdelhamid, Y., "A Novel Onsite Narrowband Tool for Flight Test Acoustic Data Processing," AIAA Paper 2002-2502, 8th AIAA/CEAS Aeroacoustics Conference & Exhibit, Breckenridge, Colorado, June 17-19, 2002. doi: 10.2514/6.2002-2502.

[12] Huang, T. S., Yang, G. J., and Tang, G. Y., "A fast two-dimensional median filtering algorithm," IEEE Transactions on Acoustics, Speech, and Signal Processing. 27 (1): 13–18. doi:10.1109/TASSP.1979.1163188.

[13] Clark, I., Nesbitt, E., Thomas, R. H., and Guo, Y., "Turbofan Aft-Radiated Broadband Acoustic Flight Effects," AIAA Paper TBD, To be presented at 30th AIAA/CEAS Aeroacoustics Conference, Rome, Italy, June 4-7, 2024.

[14] Guo, Y. and Thomas, R. H., "Geometric Acoustics for Aircraft Noise Scattering," AIAA Paper 2022-3077, 28th AIAA/CEAS Aeroacoustics Conference, Southampton, UK, June 14-17, 2022. doi: 10.2514/6.2022-3077.
[15] Czech, M. J. and Thomas, R. H., "Open Rotor Aeroacoustic Installation Effects for Conventional and Unconventional Airframes," AIAA Paper 2013-2185, 19th AIAA/CEAS Aeroacoustics Conference, Berlin, Germany, May 27-29, 2013. doi:10.2514/6.2013-2185.
[16] Kontos, K. B., Kraft, R. E., and Gliebe, P. R., "Improved NASA-ANOPP Noise Prediction Computer Code for Advanced Subsonic Propulsion Systems, Volume 2: Fan Suppression Model Development," NASA CR 202309, 1997. URL https://ntrs.nasa.gov/citations/19970005047.
[17] Clark, I., Thomas, R., and Guo, Y., "Fan Acoustic Flight Effects on the PAA & ASN Flight Test," AIAA Paper 2022-2996, 28th AIAA/CEAS Aeroacoustics Conference, Southampton, UK, June 14-17, 2022. doi: 10.2514/6.2022-2996.
[18] Wong, J., Nesbitt, E., Jones, M., and Nark, D,. "Flight Test Methodology for NASA Advanced Inlet Liner on 737MAX-7 Test Bed (Quiet Technology Demonstrator 3)," AIAA Paper 2019-2763, 25th AIAA/CEAS Aeroacoustics Conference, Delft, The Netherlands, May 20-23, 2019. doi: 10.2514/6.2019-2763.
[19] Virtanen, P., Gommers, R., Oliphant, T.E., Haberland, M., Reddy, T., Cournapeau, D., Burovski, E., Peterson, P., Weckesser, W., Bright, J., van der Walt, S. J., Brett, M., Wilson, J., Millman, K. J., Mayorov, N., Nelson, A. R. J., Jones, E., Kern, R., Larson, E., Carey, C.J., Polat, I., Feng,Y., Moore, E. M., VanderPlas, J., Laxalde, D., Perktold, J., Cimrman, R., Henriksen, I., Quintero, E. A., Harris, C. R., Archibald, A. M., Ribeiro, A. H., Pedregosa, F., and van Mulbregt, P., "SciPy 1.0: Fundamental Algorithms for Scientific Computing in Python," Nature Methods, Vol. 17, No. 3, 2020, pp. 261-272. doi: 10.1038/s41592-019-0686-2.